Comparative Medicine
Copyright 2010
by the American Association for Laboratory Animal Science

Vol 60, No 2
April 2010
Pages 96–106

Knockdown of Bicaudal C in Zebrafish (*Danio rerio*) Causes Cystic Kidneys: A Nonmammalian Model of Polycystic Kidney Disease

Denise J Bouvrette,[1] Vinoth Sittaramane,[2] Jerry R Heidel,[3] Anand Chandrasekhar,[2] and Elizabeth C Bryda[1,*]

Polycystic kidney disease (PKD) is one of the leading causes of end-stage renal disease in humans and is characterized by progressive cyst formation, renal enlargement, and abnormal tubular development. Currently, there is no cure for PKD. Although a number of PKD genes have been identified, their precise role in cystogenesis remains unclear. In the *jcpk* mouse model of PKD, mutations in the bicaudal C gene (*Bicc1*) are responsible for the cystic phenotype; however, the function of Bicc1 is unknown. In this study, we establish an alternative, nonmammalian zebrafish model to study the role of Bicc1 in PKD pathogenesis. Antisense morpholinos were used to evaluate loss of *Bicc1* function in zebrafish. The resulting morphants were examined histologically for kidney cysts and structural abnormalities. Immunostaining and fluorescent dye injection were used to evaluate pronephric cilia and kidney morphogenesis. Knockdown of zebrafish *Bicc1* expression resulted in the formation of kidney cysts; however, defects in kidney structure or pronephric cilia were not observed. Importantly, expression of mouse *Bicc1* rescues the cystic phenotype of the morphants. These results demonstrate that the function of Bicc1 in the kidney is evolutionarily conserved, thus supporting the use of zebrafish as an alternative in vivo model to study the role of mammalian Bicc1 in renal cyst formation.

Abbreviations: dpf, days postfertilization; hpf, hours postfertilization; *jcpk*, juvenile congenital polycystic kidney; KH, K homology; PKD, polycystic kidney disease; SAM, sterile α motif.

Polycystic kidney disease (PKD) is one of the leading causes of end-stage renal disease, with autosomal dominant PKD affecting 1 in every 500 to 1000 persons.[24] Autosomal dominant PKD is characterized by fluid-filled cysts in the kidneys and extrarenal abnormalities including hepatic and pancreatic cysts, hypertension, intracranial aneurysms, aortic dissection, cardiac valve abnormalities, and abdominal wall hernias.[62] The rarer recessive form of the disease, autosomal recessive PKD, occurs in approximately 1 in every 20,000 live births and is characterized by cysts in the collecting ducts, biliary dysgenesis, and hepatic fibrosis.[62] Feline PKD, which closely mimics human autosomal dominant PKD, is a prominent inherited disorder, with nearly 40% of Persian and Persian-related cats worldwide testing positive for PKD.[3,4,14] Despite advances in identifying some of the genes involved in PKD, there is currently no cure for the disorder, and the molecular pathways and mechanisms involved in cyst initiation, formation, and progression are not completely understood.

Animal models, particularly rodents, have been instrumental in the identification of genes that play a role in the development of cysts. One example is the *jcpk* mouse model in which homozygous affected animals have a phenotype that closely resembles human autosomal dominant PKD, with bilateral cysts in all parts of the nephron.[23] Mutations in *Bicc1*, the mammalian ortholog of the *Drosophila* Bicaudal C gene (*BicC*), are responsible for disease in *jcpk* model.[13] In *Drosophila*, *BicC* is required for various aspects of oogenesis and specification of anterior–posterior patterning functions.[40] Female flies heterozygous for *BicC* mutant alleles produce embryos with a range of anterior–posterior patterning defects, including bicaudal embryos. Recent reports show that BicC is a RNA-binding protein that recruits a deadenylase complex to its target RNAs and functions to regulate oogenesis, cytoskeletal rearrangements, and its own translation.[11,37,52] Interestingly, although mutations in *BicC* cause developmental defects in *Drosophila*, mutations in the mouse ortholog, *Bicc1*, do not cause developmental defects but instead lead to PKD in affected animals.

Rodent models have played an important role in the identification of genes involved in cystogenesis; however, determining the in vivo function of these genes is cumbersome due to the lack of efficient means to manipulate gene expression in living animals. Zebrafish offer an attractive alternative to rodent PKD models due to the ease of visualizing organs and tissues in the transparent embryos and juveniles, the conservation of genetic pathways regulating organogenesis, and the ability to rapidly assay loss- and gain-of-function phenotypes for any gene.

The pronephros is the first kidney to develop in vertebrates and is functional in larval zebrafish.[28] The pronephros consists of 2 fused glomeruli at the midline and paired tubules and collecting ducts, which empty into the cloaca. Although the zebrafish pronephros is more primitive than the metanephric mammalian kidney, it still contains the same specialized renal cell types in the glomerulus and tubules that are seen in the mouse. Unlike other

Received: 15 Oct 2009. Revision requested: 05 Dec 2009. Accepted: 09 Dec 2009.
[1]Genetics Area Program and Department of Veterinary Pathobiology, Research Animal Diagnostic Laboratory, College of Veterinary Medicine and [2]Division of Biological Sciences and Bond Life Sciences Center, University of Missouri, Columbia, Missouri; [3]Veterinary Diagnostic Laboratory, College of Veterinary Medicine, Oregon State University, Corvallis, Oregon.
[*]Corresponding author. Email: brydae@missouri.edu

alternative vertebrate model systems, such as *Xenopus*, zebrafish have a closed nephron system, which is more similar to the mammalian nephron.[32] The zebrafish pronephros develops within 2 d after fertilization, and morphogenetic events model those in mammalian kidney development.[20] Notably, several studies have demonstrated that mutations in zebrafish orthologs of human and mouse PKD genes result in cystic phenotypes in fish.[39,45,54]

In this study, we use the unique molecular tools and features of zebrafish to demonstrate that elimination of *bicc1* function in the zebrafish causes cyst formation. We provide evidence that the cystic phenotype can be rescued with the addition of mouse *Bicc1*. These results demonstrate that the role of the Bicc1 protein in the kidney is evolutionarily conserved and suggest that the zebrafish is an excellent in vivo model system to investigate the role of Bicc1 in kidney development and PKD pathogenesis.

Materials and Methods

Animals. Wild-type zebrafish were bred and raised inhouse by using breeding pairs that have been maintained as a closed colony for several generations. Fish were reared under the guidelines described in the *Guide for the Care and Use of Laboratory Animals*[33] and the *Zebrafish Book*.[61] The protocol for the experimental use of fish was approved by the University of Missouri Institutional Animal Care and Use Committee. Adult fish were kept in a filtered, UV-treated recirculating aquatic system at 28.5 °C on a 14:10-h light:dark cycle. The adult fish were fed brine shrimp (*Artemia nauplii*) twice daily. Fish were spawned and embryos collected by using a mesh-bottom tank system. Embryos were collected in 90-mm culture dishes in E3 embryo medium[61] and kept in an incubator at 28.5 °C for 4 d postfertilization (dpf). At 4 dpf, embryos were fed live paramecia (*Paramecia multimicronucleatum*) twice daily. At 9 dpf, embryos were moved to baby-rearing containers in the nursery and fed both paramecia and brine shrimp twice daily. Containers were cleaned carefully and replaced with clean system water twice daily. The proportion of brine shrimp was increased gradually while phasing out the paramecia until 21 dpf, at which point progeny were moved to adult tanks and fed live brine shrimp twice daily. Throughout the text, the developmental age of the embryos corresponds to the hours elapsed since fertilization (hours postfertilization [hpf] at 28.5 °C).

cDNA and sequence analysis. A construct containing the full-length wild-type mouse *Bicc1* (GenBank accession no. NM_031397) cDNA in pCS2$^+$ was kindly provided by Oliver Wessely (Louisiana State University Health Sciences Center, Baton Rouge, LA). A zebrafish ortholog of mouse *Bicc1* was identified by using Basic Local Alignment Search Tool (BLAST)[2] and designated *bicc1a*. Multiple sequence alignments were performed by using Clustal W2,[10] and the images were viewed by using Jalview.[10,12] The following nucleotide (and protein) accession numbers were used: zebrafish *bicc1a*, NM_203420 (NP_981965); mouse *Bicc1*, NM_031397 (NP_113574); and human *BICC1*, ENST000000373886 (ENSP000000362993). Conserved protein domains were identified by using multiple programs available at ExPASy,[25] including MotifScan, ProSite, and Pfam.[17,22,31,46,66]

RNA isolation and RT-PCR. Total RNA was isolated from 20 to 30 dechorinated embryos at multiple stages of development using TRIZOL reagent (Invitrogen, Carlsbad, CA). Embryos less than 30 hpf were lysed by vortexing vigorously for 2 to 3 min; embryos at least 30 hpf were sonicated on ice in 5-s bursts for 1 min. RNA pellets were washed once with 75% ethanol and resuspended in RNA storage solution (Ambion, Austin, TX). One-step RT-PCR was performed (Superscript III, Invitrogen) according to the manufacturer's instructions. Gene-specific primers for *bicc1a* (5′ CAT GAC TGC AAA CAC TCC TTT GT 3′ and 5′ AAG GTC ACG CTT CTC TGC AT 3′) were designed by using Primer3.[48] The primers used for the housekeeping gene *ef1*α were 5′ TCA CCC TGG GAG TGA AAC AGC 3′ and 5′ ACT TGC AGG CGA TGT GAG CAG 3′.[30] A 25-µL reaction containing 100 ng template RNA and 0.2 µM gene-specific primers was amplified under the following conditions: 45 °C for 30 min; 94 °C for 2 min; 40 cycles of 94 °C for 30 s, 58.5 °C (*bicc1a*) or 66 °C (*ef1*α) for 30 s, 68 °C for 1 min, with a final extension of 7 min at 68 °C. After PCR, 15 µL of the amplified products were separated on a 3% agarose (in Tris-borate–EDTA) gel. Expected products of 179 bp for *bicc1a* and 648 bp for *ef1*α were visible after separation by gel electrophoresis.

Morpholinos. Translation-blocking or splice-blocking antisense morpholino oligonucleotides were designed by Gene Tools (Philomath, OR) and obtained from Open Biosystems (Huntsville, AL). The sequences for the morpholinos used are as follows: *bicc1a* translation-blocking (NM_203420), 5′ TCT CTG AGG CCG CCA TAG CAA GAC T3′; *bicc1a* splice-blocking, 5′ GGA AGC ATG ACT TTC CTC ACC TTT C 3′; and *pkd2* translation-blocking (AY618926), 5′ AGG ACG AAC GCG ACT GGA GCT CAT C 3′.[54] A g*li2* antisense mismatch morpholino (5′ CCT CTT ACC TCA GTT ACA ATT TAT A 3′) was used as a control.[35]

RNA and morpholino injections. The *mBicc1*–pCS2+ construct was linearized with *Not*I (New England Biolabs, Ipswich, MA) and full-length synthetic mouse *Bicc1* mRNA was synthesized by using mMessage mMachine (Ambion) according to the manufacturer's instructions. Antisense morpholinos and mRNA were suspended in Danieau buffer[43] containing 0.1% phenol red, loaded into microcapillary needles (Stoelting, Wood Dale, IL), and injected into 1- to 4-cell embryos by using a microinjector (ASI, Eugene, OR). Dose–response experiments indicated that effective dose ranges were 1 to 20 ng for morpholino oligonucleotides and 150 to 750 pg for RNA rescue studies. At higher doses of morpholino oligonucleotides, the injected embryos exhibited nonspecific defects and died. Similarly, dose–response experiments defined the highest RNA dose at which nonspecific or toxic effects were absent.

Immunohistochemistry and in situ hybridization. Whole-mount immunohistochemistry was performed as described previously[6] with the following modifications. Embryos were fixed overnight in Dent[18] (80% methanol, 20% DMSO), treated with 10% H_2O_2 in Dent for 2 h, and placed in 100% methanol. A monoclonal antibody against the chicken α1 subunit of Na^+-K^+ ATPase[55] was acquired from the Developmental Studies Hybridoma Bank (Iowa City, IA) and used at a 1:10 dilution. Synthesis of the digoxigenin-labeled probes and whole-mount in situ hybridization were carried out as described previously.[5] The probes used for in situ hybridization were derived from EST clone AL923800 (clone ID 131-B03-2, OpenBiosystems) and linearized with *Xho*I (antisense; New England Biolabs) or *Xba*I (sense; New England Biolabs). Sense and antisense digoxigenin–dUTP-labeled probes were synthesized by using DIG RNA labeling mix (Roche Applied Science, Indianapolis, IN) according to the manufacturer's instructions, with 1 µg linearized plasmid DNA template and either T3 (antisense) or T7 (sense) RNA polymerase. Embryos were deyolked as necessary, mounted in 70% glycerol, and examined by fluo-

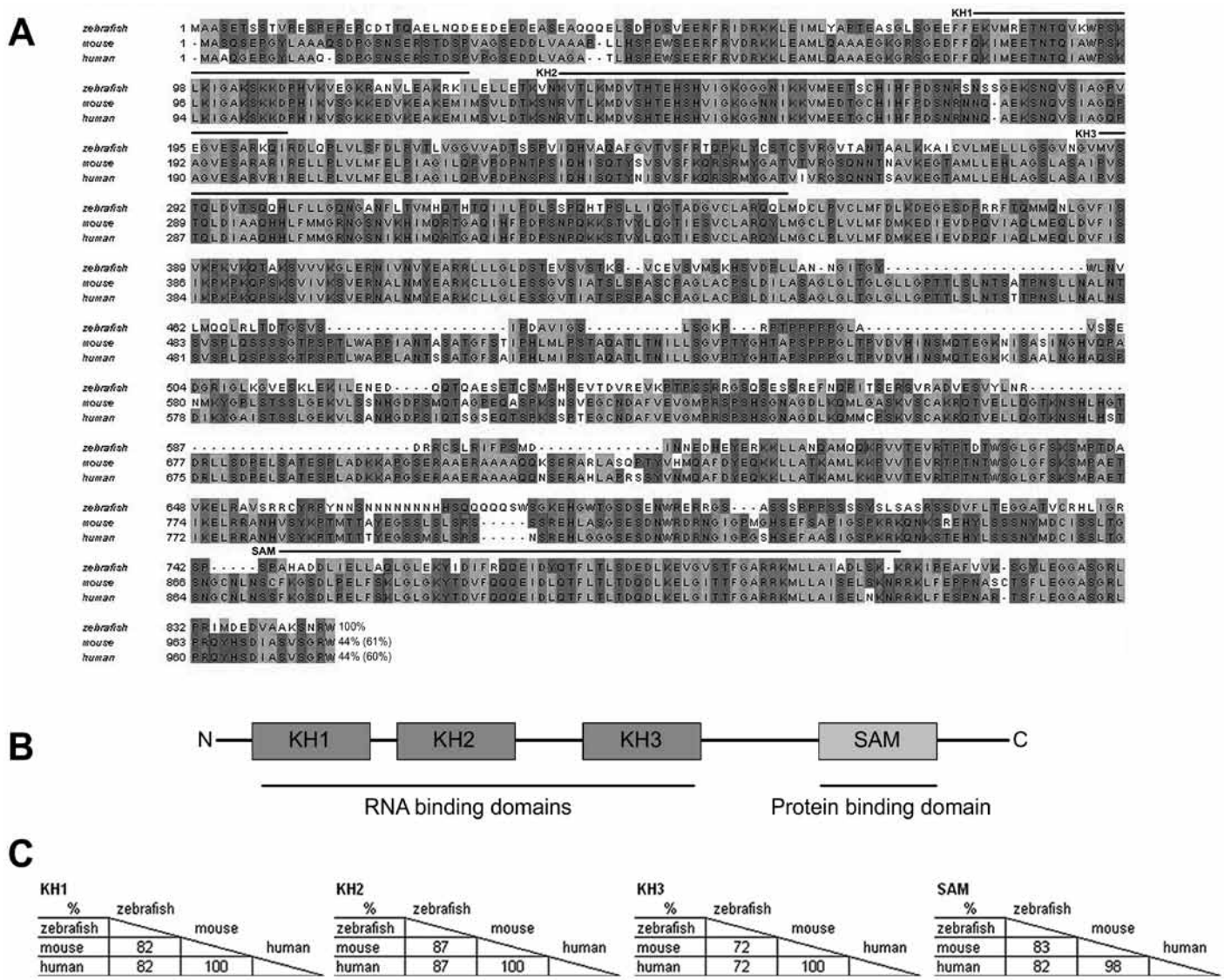

C

KH1

%	zebrafish	mouse	human
zebrafish			
mouse	82		
human	82	100	

KH2

%	zebrafish	mouse	human
zebrafish			
mouse	87		
human	87	100	

KH3

%	zebrafish	mouse	human
zebrafish			
mouse	72		
human	72	100	

SAM

%	zebrafish	mouse	human
zebrafish			
mouse	83		
human	82	98	

Figure 1. Bicaudal C (Bicc1) protein comparison. (A) Comparison of zebrafish, mouse, and human Bicc1 protein sequences. The number immediately after the peptide sequences represents the percentage identity of that sequence compared with the zebrafish sequence, and the number in parentheses represents the overall conservation of the peptide sequence compared with the zebrafish sequence. Light gray blocks of amino acids indicate residues that are conserved between at least 2 of the species, whereas dark gray blocks of amino acids represent residues that are conserved among all 3 species. (B) Schematic of the predicted Bicc1 protein and its functional domains. (C) Comparison of human, mouse, and zebrafish amino acid sequences for Bicc1 functional domains. The percentages of amino acid conservation for the 3 KH domains and the SAM domain are listed.

rescence microscopy (BX60, Olympus, Center Valley, PA). In all comparisons, at least 8 embryos for each category were examined.

Histologic analysis. Five-day-old larvae were fixed overnight in 2% glutaraldehyde, 2% paraformaldehyde in 0.1 M sodium cadodylate buffer, pH 7.35. Samples were washed in cadodylate buffer, taken through an ethanol dehydration series, embedded in JB4 (Polysciences, Warrington, PA), and serially sectioned at 4 µm by using a microtome (Ultracut UCT, Leica, Bannockburn, WI). Slides were stained with 1% alkaline toluidine blue in 1% sodium borate[8,42] and observed by light microscopy (Axiophot, Zeiss, Thornwood, NY). Images were acquired with an Olympus DP70 digital camera. In all comparisons, at least 6 embryos for each category were examined.

Rhodamine–dextran dye injections. Rhodamine–dextran injections were performed as previously described[36] with the following modifications. Embryos (3 to 3.5 dpf) were anesthetized with 0.02% MS222 (Tricaine, Sigma–Aldrich, St Louis, MO) and mounted on slides in 3% methylcellulose (Sigma). A 5% solution of 70-kDa tetramethylrhodamine–dextran (Invitrogen) was injected into the common cardinal vein; the embryo was covered with a coverslip and examined by using fluorescence microscopy (BX60, Olympus). Ten wild-type embryos and 8 *bicc1a* morphants were examined.

Immunostaining of cilia. Embryos (28 to 30 hpf) were fixed in Dent overnight, slowly rehydrated in PBS containing 1% DMSO and 0.1% Tween, and blocked 2 h in PBS containing 1% DMSO, 0.1% Tween, and 10% normal goat serum. Primary antibody

(mouse antiacetylated α tubulin; dilution factor, 1:400; T6793, Sigma) was added to PBS containing 1% DMSO, 0.1% Tween, and 1% normal goat serum and incubated overnight. Samples were washed 5 times for 30 min in PBS containing 1% DMSO, 0.1% Tween, and 1% normal goat serum with agitation. Secondary antibody (dilution factor, 1:500; Alexa-Fluor-568–conjugated goat antimouse, Molecular Probes, Invitrogen) was added and incubated overnight. Nuclei were counterstained with 4′,6-diamidino-2-phenylindole (Roche Applied Science) at a final concentration of 13 μM. Samples were washed 5 times for 30 min each and mounted in 70% glycerol. Whole mounts were examined by using a 2-photon point-scanning confocal microscope (LSM 510 META NLO, Zeiss). Six wild-type embryos and 5 *bicc1a* morphants were examined.

Results

Characterization of a zebrafish *bicc1* ortholog. Using the Basic Local Alignment Search Tool (BLAST),[2] we compared the mouse *Bicc1* (GenBank accession no., NM_031397) nucleotide sequence with sequences in the public database at the National Center for Biotechnology Information (NCBI) and identified a zebrafish *bicc1* ortholog (NM_203420; designated here as *bicc1a*). This *bicc1a* ortholog maps to zebrafish chromosome 14 (Ensembl assembly, Zv8) and shares 24% overall nucleotide identity with mouse *Bicc1.* The *bicc1a* transcript is approximately 2950 bp in length and encodes a protein consisting of 849 amino acids (Figure 1 A).

The zebrafish Bicc1a predicted peptide sequence contains 2 conserved functional domains: 3 K homology (KH) domains in tandem near the N terminus, and a C-terminal sterile α motif (SAM; Figure 1 B). KH domains bind RNA, whereas SAM domains have been implicated in protein–protein interactions during development.[1,50] Overall, the mouse, human, and zebrafish Bicc1 protein sequences share 44% amino-acid identity (Figure 1 A). The level of amino-acid conservation is markedly higher in the KH and SAM domains across all 3 species: 82% in KH1, 87% in KH2, 72% in KH3, and 82% in SAM (Figure 1 C). These data strongly suggest that the functional domains are vital for Bicc1 function.

Zebrafish *bicc1a* is expressed throughout early development. To determine the temporal expression pattern of *bicc1a* in the developing zebrafish embryo, we performed RT-PCR by using total RNA from embryos ranging in age from 1 to 72 hpf. The constitutively expressed gene elongation factor α (*ef1α*) served as a control.[30] *bicc1a* transcripts were present in all stages tested (Figure 2 A). Expression at the 4- to 8-cell stage (1 hpf) is due to maternally contributed *bicc1a* transcripts, consistent with *BicC* expression in *Drosophila* and *Xenopus*.[40,59] These results indicate that zebrafish *bicc1a* is expressed continuously during the period that coincides with pronephros development.

To determine the spatial expression pattern of *bicc1a*, we performed whole-mount in situ hybridization on 12- to 48-hpf embryos. A digoxigenin-labeled probe derived from EST clone AL923800, which contains the nucleotide sequence near the 5′ end of *bicc1a* and includes part of the KH domains, was used. Signal corresponding to *bicc1a* transcripts was observed in 10- to 18-hpf embryos in the developing pronephric ducts as well as at the midbrain–hindbrain boundary (Figure 2 B, C).

Knockdown of *bicc1a* generates kidney cyst-associated morphologic defects. To test whether bicc1a plays a role in kidney development and physiology, we examined the effects of loss of *bicc1a*

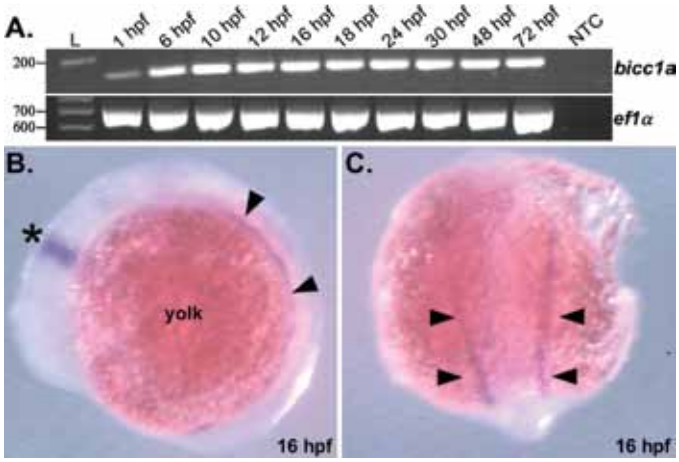

Figure 2. Gene expression of *bicc1a* in whole embryos. (A) Primers specific for zebrafish *bicc1a* or *ef1α* (control) were used in RT-PCR to amplify total RNA from whole embryos at time points from 1 h postfertilization (hpf) to 72 hpf. Amplicon sizes are 179 bp for *bicc1a* (upper panel) and 648 bp for *ef1α* (lower panel). L is a 1-kb ladder molecular size standard (Promega, Madison, WI), and NTC indicates no-template control (negative control). (B) Whole-mount in situ hybridization of 16-hpf embryo. In this lateral view, *bicc1a* expression is seen at the midbrain–hindbrain boundary (asterisk) and in the developing pronephric duct (arrowheads). (C) Dorsal view of the same embryo, with *bicc1a* expression seen bilaterally in both pronephric ducts (arrowheads).

expression by using antisense morpholino oligonucleotides.[43] Initially, dose–response experiments were performed to determine the concentration range in which specific, nontoxic effects could be obtained. As a positive control, we used a morpholino oligonucleotide against *pkd2* that previously led to kidney cysts in zebrafish.[54] Injection of *bicc1a* morpholino oligonucleotides over a broad concentration range (1 to 20 ng/embryo) induced dorsal curvature in the trunk and tail, with the severity of phenotype directly proportional to the dose (Figure 3 D through F; Table 1). Importantly, the abnormal morphology observed in the *bicc1a* morphants is similar to the phenotype of *pkd2* morpholino-injected embryos (Figure 3 C) and is a feature consistently observed in other cystic zebrafish mutants and morphants.[21,43,54] In contrast, uninjected and control oligonucleotide-injected embryos developed normally (Figure 3 A, B). At a dose of 2.5 ng or higher, the trunk phenotype was fully penetrant, with 100% of embryos exhibiting dorsal curvature (Table 1). Morpholino-injected embryos exhibited no morphologic defects up to 30 hpf. The trunk phenotype became visible by 40 hpf and was fully expressed by 48 to 60 hpf, suggesting that this phenotype is a specific effect of morpholino oligonucleotide injection. Many embryos also exhibited various degrees of pericardial edema, but the penetrance of this phenotype was variable between experiments, ranging from 0% to 50%. Therefore, only the trunk phenotype was used as a reliable indicator of *bicc1a* morphant activity in all subsequent experiments.

Renal cysts develop in *bicc1a* morphants. Although the morphologic defects of *bicc1a* morphants resemble those previously described in zebrafish mutants and morphants for PKD-causing genes, kidney cysts were not visible grossly in live *bicc1a* morphant embryos.[20,54] Therefore, we examined cross-sections of 5-d-old zebrafish embedded in JB4 for structural defects in the larval pronephros. In uninjected embryos, the glomerulus and

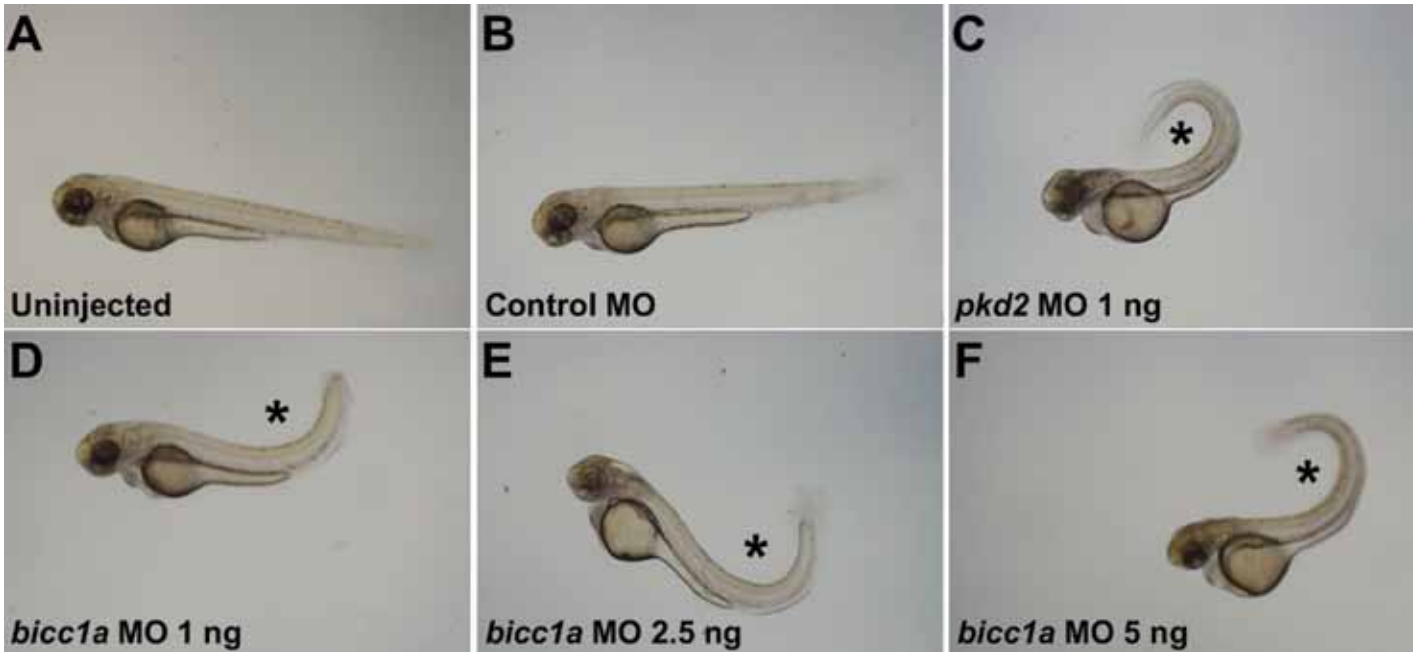

Figure 3. Morphologic defects in *bicc1a* morphant embryos. Panels show bright-field images of 72-hpf embryos (magnification, ×250). (A) Uninjected fish (control). (B) Control morpholino (MO). (C) *pkd2* MO at 1-ng dose. (D) *bicc1a* MO at 1-ng dose. (E) *bicc1a* MO at 2.5-ng dose. (F) *bicc1a* MO at 5-ng dose. No gross abnormalities were detected in uninjected animals or those injected with the control MO. In contrast, embryos injected with the *pkd2* or *bicc1a* MO showed pronounced dorsal curvature of the trunk (asterisk).

Table 1. Phenotypes observed in morpholino studies using a translation-blocking oligonucleotide toward *bicc1a*

	Dorsal curvature			Kidney cysts	
	% affected	total no. embryos evaluated	no. of experiments	no. of embryos affected	total no. embryos evaluated
Uninjected	0	266	7	0	10
Control MO 1 ng	5.3	112	4	0	4
bicc1a MO 1 ng	96.5	29	1	5	5
bicc1a MO 2.5 ng	100	265	7	13	13
bicc1a MO 5 ng	100	84	3	8	8
bicc1a MO 10 ng	100	84	3	not available	
bicc1a MO 20 ng	100	18	1	not available	
pkd2 MO 1 ng	100	87	3	14	14
Bicc1 RNA 150 pg	21.6	37	1	0	4

MO, morpholino oligonucleotide

pronephric tubules were normal (Figure 4 A, B), with cellular morphologies resembling those described previously for wild-type embryos.[19,21] In contrast, *bicc1a* morphants had prominent cysts in the pronephric tubules as well as cystic dilations in the glomerulus and pronephric ducts (Figure 4 C through F). The cysts were lined by epithelial cells, which appeared normal. The cysts were noted in every *bicc1a* morphant embryo examined (n = 18). These results demonstrate that abrogation of *bicc1a* expression leads to the formation of cysts in the developing pronephros. Importantly, similar gross morphology and cystic defects were observed by using a second *bicc1a* morpholino designed to target the splice junction between exons 2 and 3 of *bicc1a.*(Table 2). This splice-blocking morpholino results in a transcript that mimics the defective transcript in the *jcpk* mouse. The observation that 2 independent morpholinos targeting the same gene induce a similar phenotype strongly suggests that the formation of pronephric cysts is specific to the loss of *bicc1a* function.

Kidney morphogenesis and function appear normal in *bicc1a* morphants. To test whether the formation of cysts in *bicc1a* morphants was accompanied by changes in kidney development and physiology, we stained 48-hpf embryos with anti-Na^+-K^+ ATPase α subunit monoclonal antibody α6F, which labels the pronephric ducts and tubules.[21] The morphology and arrangement of these structures was not affected in *bicc1a* morphants (Figure 5 A, B), indicating that cyst formation does not result from aberrant development of the pronephros.

Disruption or blockage of fluid flow can result in the formation of cysts in the pronephric kidney.[36] To determine whether the formation of cysts in *bicc1a* morphants was the result of blocked fluid flow through the pronephros, we examined the excretion of

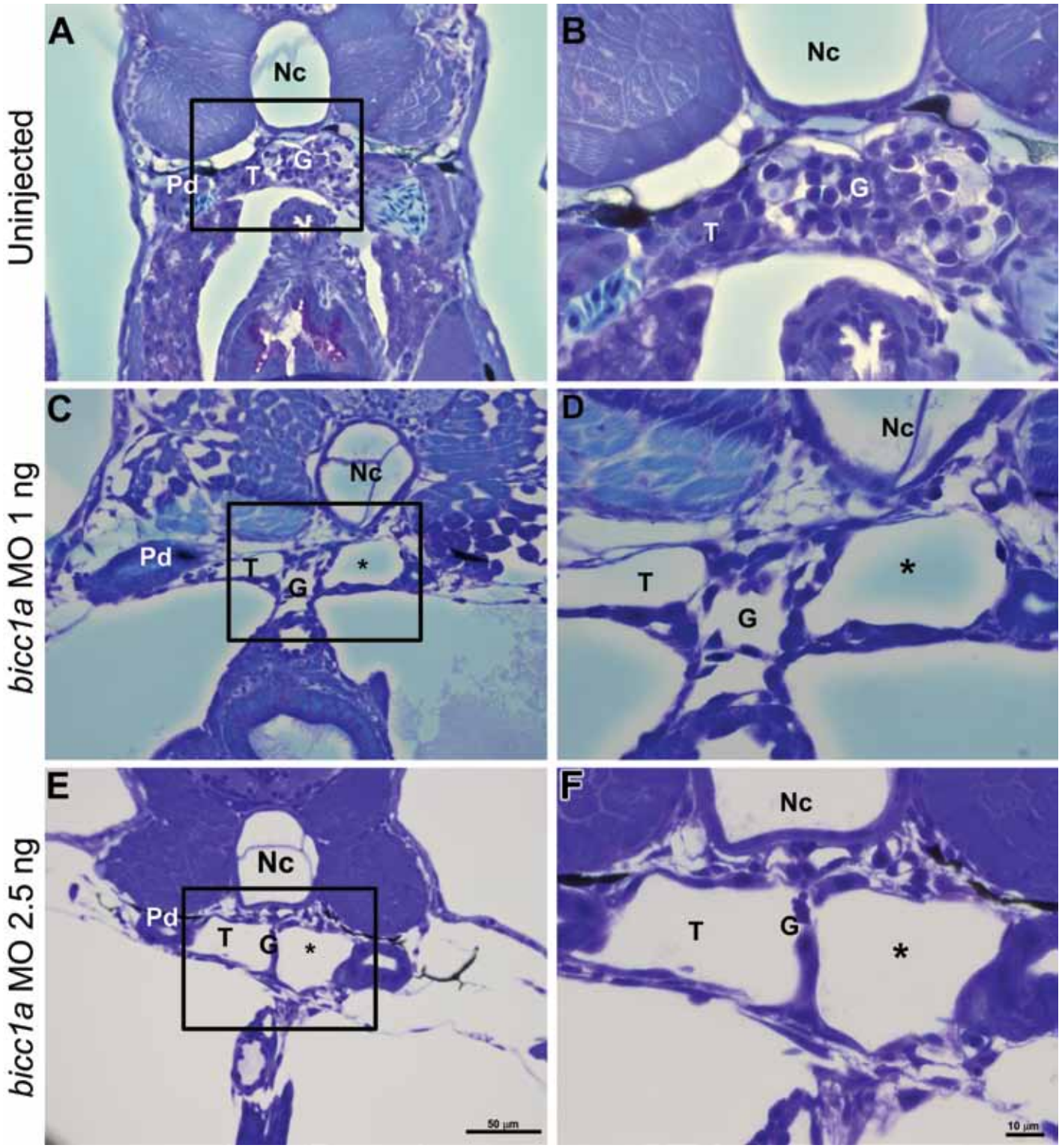

Figure 4. Kidney cysts in *bicc1a* morphant embryos. Histologic analysis of cross-sections from 5-d-old embryos. (A) Control morphant; magnification, ×400. (B) Boxed area in panel A; magnification, ×1000. (C) *bicc1a* morphant at 1-ng dose of *bicc1a* MO; magnification, ×400. (D) Boxed area from panel C; magnification, ×1000. (E) *bicc1a* morphant at 2.5-ng dose of *bicc1a* MO; magnification, ×400. (F) Boxed area from panel E; magnification, ×1000. Nc, notochord; Pd, pronephric duct; T, pronephric tubule; G, glomerulus; asterisks, cysts. Sections are representative of embryos examined (control MO, n = 6; uninjected, n = 8; *bicc1a* morphants, n = 18). Scale bar, 50 µm (panels A, C, and E); 10 µm (panels B, D, and F).

Table 2. Phenotypes observed in morpholino studies using a splice-blocking oligonucleotide toward *bicc1a*

	Dorsal curvature			Kidney cysts	
	% affected	total no. embryos evaluated	no. of experiments	no. of embryos affected	total no. embryos evaluated
Uninjected	0	102	3	0	8
Control MO 1 ng	4	51	3	0	3
bicc1a MO 2.5 ng	52	69	2	not available	
bicc1a MO 5 ng	59	85	3	not available	
bicc1a MO 10 ng	80	99	3	5	5

MO, morpholino oligonucleotide

rhodamine–dextran from the cloaca immediately after injection into the common cardinal vein of 3- to 3.5-d-old larvae. In control animals (n = 10), boli of fluorescent material were excreted within 2 to 3 min of injection (Figure 5 C). Rhodamine–dextran also was excreted efficiently by *bicc1a* morphants (n = 8; Figure 5 D), although the process was slightly slower than in controls, with excretion between 5 to 8 min of injection. These results suggest strongly that the formation of cysts in *bicc1a* morphants does not interfere with pronephric fluid flow.

A number of PKD-causing genes encode proteins that localize to the primary cilia of renal epithelial cells, suggesting that cilia structure or function plays an important role in the formation of cysts.[15,16,27,29,34,38,41,45,47,51,56,60,63-65,67] To determine whether the primary cilia are affected in *bicc1a* morphants, we performed immunostaining using a mouse antiacetylated-α-tubulin monoclonal antibody in 28- to 30-hpf wild-type and *bicc1a* morphant embryos. Confocal fluorescence microscopy revealed that the length, number, and direction of the cilia in *bicc1a* morphants (n = 5) closely resembled that of the wild type controls (n = 6; Figure 5 E, F). Taken together, these results indicate that the formation of cysts in *bicc1a* morphants is not due to overt defects in pronephros development, defects in cilia formation or structure, or inhibition of fluid flow through the pronephros.

Expression of mouse *Bicc1* can prevent cyst formation in zebrafish *bicc1a* morphants. To further demonstrate that pronephric cysts in *bicc1a* morphants are specifically due to the knockdown of *bicc1a*, we tested whether expression of the mouse *Bicc1* ortholog could rescue the cystic phenotype in zebrafish. Synthetic full-length mRNA encoding mouse *Bicc1* that lacks the *bicc1a* morpholino-binding site was coinjected with *bicc1a* morpholino oligonucleotide and embryos were examined histologically for morphologic defects and cyst formation (Figure 6, Table 1). Uninjected and mouse *Bicc1* mRNA-injected embryos were indistinguishable up to 5 dpf (Figure 6 A, B, E, F), indicating that injection of mouse *Bicc1* mRNA alone has no detrimental effects on larval development or physiology. In embryos coinjected with both the *bicc1a* morpholino oligonucleotide and mouse *Bicc1* mRNA, the occurrence of dorsal trunk curvature was markedly reduced (Figure 6 D), occurring in approximately 60% fewer embryos than those injected with the *bicc1a* oligonucleotide alone (Figure 6 C). Histologic examination of coinjected embryos (n = 6) revealed reversal of the cystic phenotype, with the embryos more closely resembling the uninjected controls rather than the *bicc1a* morphants (Figure 6 E, G, H). The ability of mouse *Bicc1* to rescue the cystic morphants strongly suggests that the formation of renal cysts in *bicc1a* morphants is a direct result of the loss of *bicc1a* and demonstrates that the functional role of Bicc1 is conserved in mouse and zebrafish.

Discussion

The utility of zebrafish as a model for PKD has been demonstrated in several studies in which PKD-causing genes in mammals, including *Pkd2*, *Nek8*, and *Invs*, have been shown to cause cyst formation in the zebrafish pronephros.[39,45,54] In addition, in several independent genetic screens, at least 20 zebrafish pronephric mutants have been recovered that include cyst formation as a component of their phenotype.[9,21,26] The relatively short developmental cycle of zebrafish and the abilities to readily visualize organs and tissues, test drugs by their addition to the water, and rapidly assay gain- or loss-of-function phenotypes make zebrafish an attractive animal system for studying kidney development and function. The developmental similarities between the zebrafish pronephros and the mammalian kidney are well-established, further strengthening the utility of zebrafish as a nonmammalian model for study of the kidney.

Our data validate the use of a *bicc1a* zebrafish model as a complementary alternative system in which to study the role of Bicc1 in cystogenesis. A primary goal of this study was to demonstrate conservation of Bicc1 function in the kidneys of zebrafish and mice. We show that the morpholino-induced loss of zebrafish *bicc1a* results in abnormal morphology and kidney cyst formation. The consequence of the mutation in the *jcpk* mouse PKD model is a severely truncated protein missing both the KH and SAM domains, and this protein is expected to be functionally null.[13] Knockdown of zebrafish *bicc1a* presumably decreases the amount of Bicc1a protein, closely mimicking the situation seen in *jcpk* homozygous mice. Similar to the phenotype in *jcpk* mice, *bicc1a* morphant fish exhibit cysts in all parts of the nephron, including the glomerulus.

In the current study, we used 2 distinct morpholinos that specifically targeted *bicc1a*. Both yielded similar phenotypes, suggesting that the cystic phenotypes are a direct result of the loss of *bicc1a* function. Importantly, the cystic phenotype can be reversed with the addition of mouse *Bicc1.* These data provide further evidence that cyst formation in *bicc1a* morphants is due to knockdown of *bicc1a* and that the function of Bicc1 in the kidney is conserved.

Many genes involved in PKD code for proteins that localize to the primary cilia or basal body, suggesting that normal ciliogenesis and normal ciliary structure, and function are important for proper kidney morphogenesis and maintenance.[15,16,27,29,34,38,41,45,47,51,56,60,63-65,67] Likewise, several cystic zebrafish mutants are due to defects in genes known to be involved in ciliary structure or function.[36,44,47,54,60] Electron microscopic studies of *jcpk* homozygous mice reveal morphologically normal cilia present on the apical surface of the renal epithelial cells (data not shown), and the mouse Bicc1 protein does not localize to the primary cilia of mouse inner medullary collecting duct cells.[53] In addition,

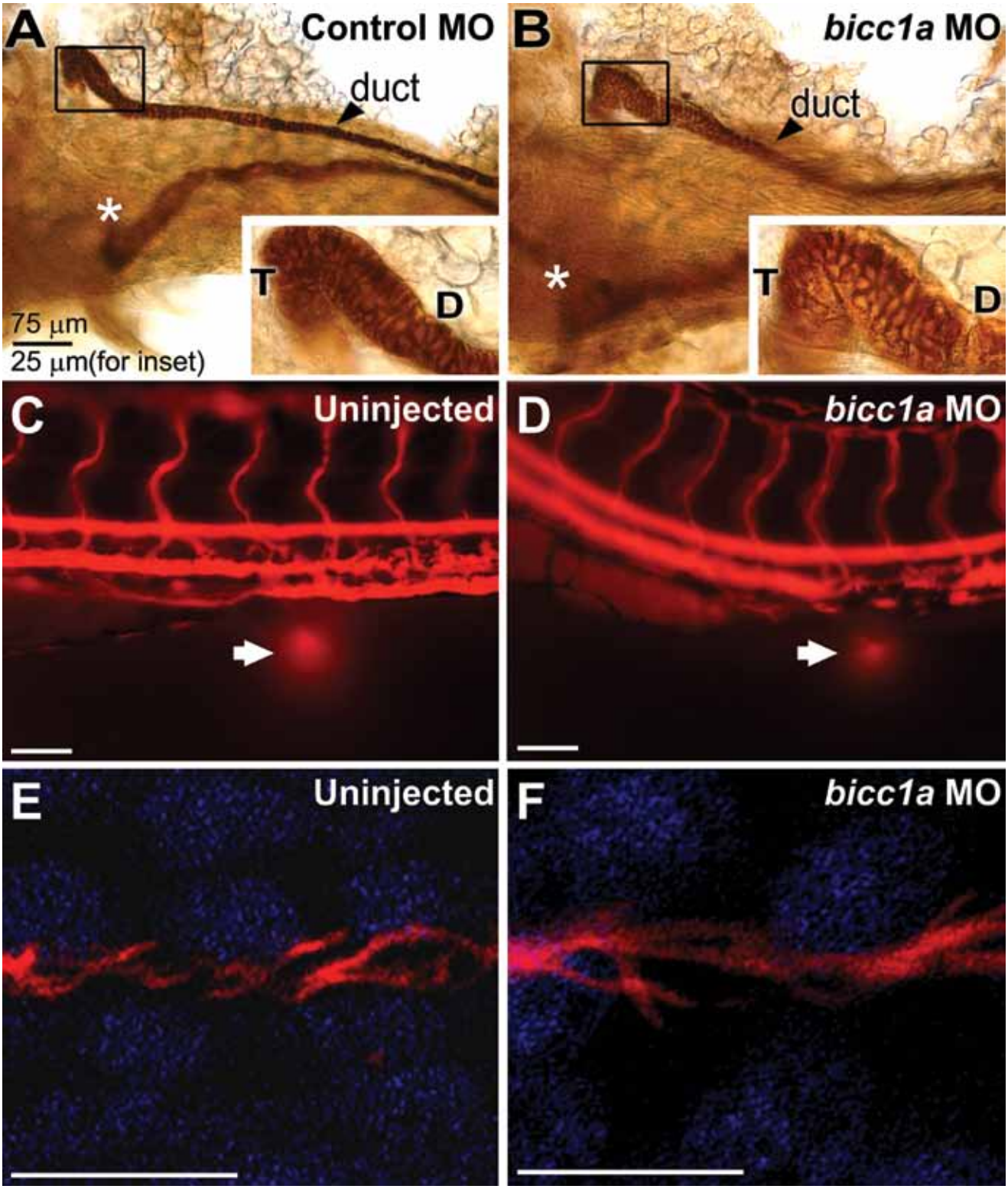

Figure 5. Kidney morphogenesis and function. The upper panels show whole-mount immunostaining of 72-hpf embryos with α6F antibody. Embryos were (A) injected with the control MO or (B) injected with *bicc1a* MO. Both panels A and B are dorsal views, with anterior to the left. The arrowhead indicates a duct, and the asterisk indicates the location of a paired tubule (out of focus). D, duct; T, tubule. The boxed region (magnification, ×2000) is magnified in the inset (magnification, ×600. A total of 8 embryos were examined in each group, and representative embryos are depicted. (C) Uninjected wild type control (n = 10) and (D) *bicc1a* morphant (n = 8) animals injected with fluorescently labeled dextran; magnification, ×400. Arrows indicate excretion of the labeled dextran from the cloaca by way of the pronephros. Confocal microscopy (magnification, ×400 with ×3 optical zoom) images of pronephric cilia in 28- to 30-hpf (E) wild-type (n = 5) and (F) *bicc1a* morphant (n = 6) embryos. Scale bar, 50 μm (panels C and D); 10 μm (panels E and F).

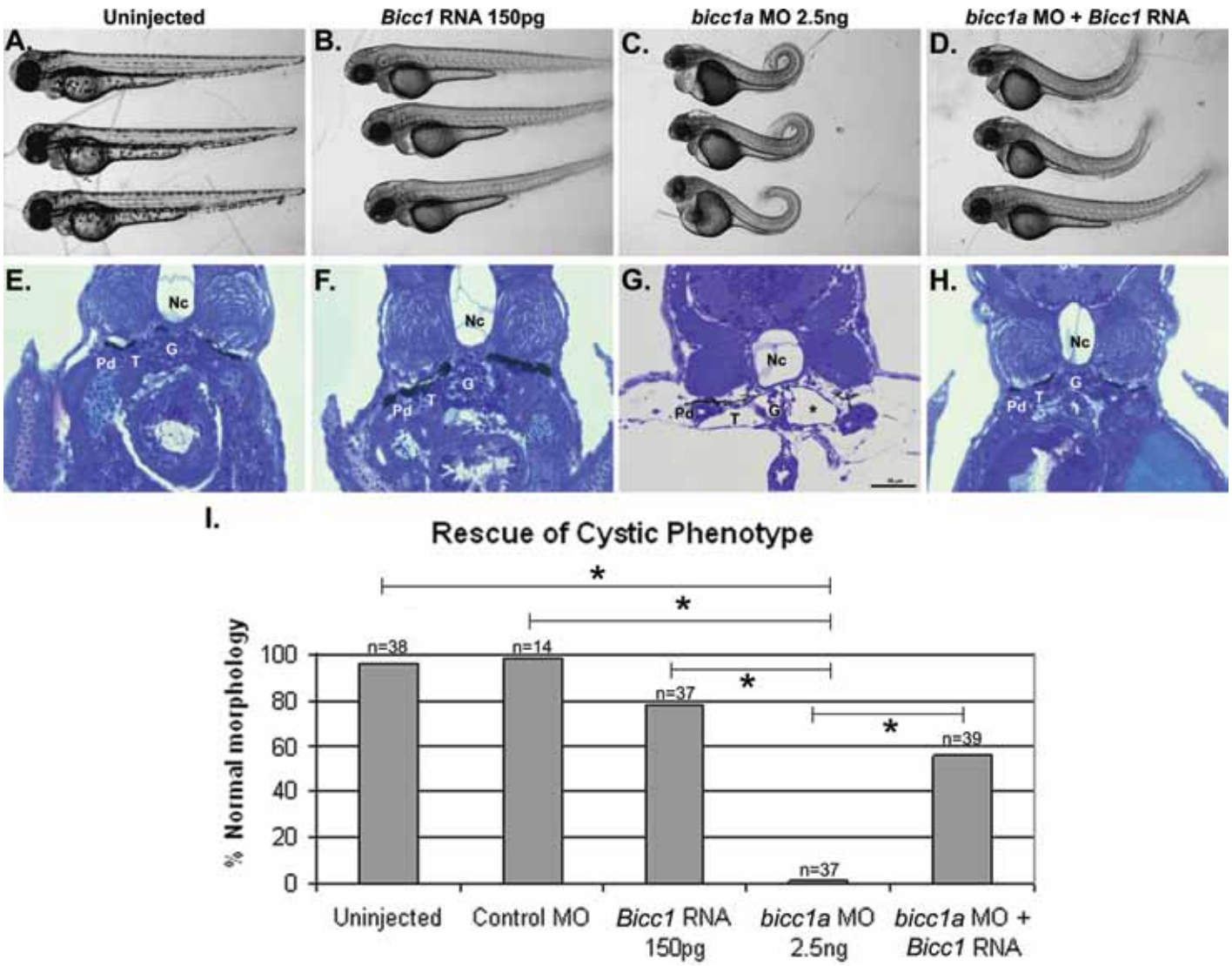

Figure 6. Mouse Bicc1 rescues the zebrafish bicc1a morphant phenotype. Bright-field images (magnification, ×250) of representative embryos that were (A) uninjected, (B) injected with 150 pg mouse *Bicc1* RNA, (C) injected with 2.5 ng zebrafish *bicc1a* MO, or (D) coinjected with 150 pg mouse *Bicc1* RNA and 2.5 ng zebrafish *bicc1a* MO. Embryos injected with the *bicc1a* MO showed pronounced dorsal curvature of the trunk (C). Panels E through H show the histologic analysis of cross-sections of representative fish from each treatment group; magnification, ×400. Nc, notochord; Pd, pronephric duct; T, pronephric tubule; G, glomerulus; asterisks, cysts. Scale bar, 50 µm (E through H). (I) Histogram of the number and percentage of animals observed in each group exhibiting normal outward morphology. In the morphants that were coinjected with mouse *Bicc1* RNA and *bicc1a* MO, 56% did not exhibit outward morphologic defects and showed little or no dorsal curvature of the trunk. Statistical analysis using Fisher's Exact nonparametric test[7] (Sigma Plot) showed a significant difference (*, $P < 0.05$) between groups.

Xenopus embryos injected with morpholinos to knockdown expression of *xBicC* display a cystic phenotype but do not have any obvious differences in the number or length of cilia.[57] Likewise, assessment of the pronephric cilia in zebrafish *bicc1a* morphants revealed no apparent defects in cilia, and fluid flow through the pronephros was not compromised. Given all these independent data, we propose that Bicc1 is not involved directly in the structure or formation of cilia but instead acts in a downstream or parallel pathway that, when perturbed, leads to cystogenesis.

Drosophila BicC localizes RNA and regulates translation by interacting with components of the polyadenylation machinery and associating with specific mRNAs, including the 5′ untranslated region of its own mRNA.[11,37,49,52] Studies in *Xenopus* suggest that the KH RNA-binding domains are important for Bicc1 function in the pronephros.[57] Bicaudal C binds RNA through its KH domains,[11,37,49,52] and a recent report indicates that *Xenopus* Bicc1 functions to repress translation of the PKD-protein polycystin 2.[58] Our previous work has demonstrated that Bicc1 interacts with another PKD-related protein, SamCystin, in a RNA-dependent manner,[53] however, the precise molecular function of mammalian Bicc1 in the kidney remains unclear. The ability to exploit the zebrafish as an alternative model system in which to study Bicc1 specifically in the kidney will allow us to readily and rapidly determine the functional role of Bicc1 in cyst formation and PKD pathogenesis.

Acknowledgments

We thank Dr Craig Franklin for critical reading of the manuscript, Amy Foerstel and Moe Baccam for assistance with fish care, and Heath Berg for technical assistance. This work was supported in part by grants from The American Society of Nephrology (M James Scherbenske Grant to ECB), NIH NS40449 (to AC), the University of Missouri College of Veterinary Medicine (to ECB), and the University of Missouri Department of Veterinary Pathobiology (to DJB). DJB was supported by the University of Missouri Life Sciences Predoctoral Fellowship program.

References

1. **Adinolfi S, Bagni C, Castiglione Morelli MA, Fraternali F, Musco G, Pastore A.** 1999. Novel RNA-binding motif: the KH module. Biopolymers **51:**153–164.
2. **Altschul SF, Gish W, Miller W, Myers EW, Lipman DJ.** 1990. Basic local alignment search tool. J Mol Biol **215:**403–410.
3. **Barrs VR, Gunew M, Foster SF, Beatty JA, Malik R.** 2001. Prevalence of autosomal dominant polycystic kidney disease in Persian cats and related-breeds in Sydney and Brisbane. Aust Vet J **79:**257–259.
4. **Biller DS, DiBartola SP, Eaton KA, Pflueger S, Wellman ML, Radin MJ.** 1996. Inheritance of polycystic kidney disease in Persian cats. J Hered **87:**1–5.
5. **Bingham S, Chaudhari S, Vanderlaan G, Itoh M, Chitnis A, Chandrasekhar A.** 2003. Neurogenic phenotype of mind bomb mutants leads to severe patterning defects in the zebrafish hindbrain. Dev Dyn **228:**451–463.
6. **Bingham S, Higashijima S, Okamoto H, Chandrasekhar A.** 2002. The zebrafish trilobite gene is essential for tangential migration of branchiomotor neurons. Dev Biol **242:**149–160.
7. **Blevins L, McDonald CJ.** 1985. Fisher's exact test: an easy-to-use statistical test for comparing outcomes. MD Comput **2:**15–19, 68.
8. **Burns WA.** 1978. Thick sections: technique and applications, ch 4. New York (NY): John Wiley and Sons.
9. **Chen JN, Haffter P, Odenthal J, Vogelsang E, Brand M, van Eeden FJ, Furutani-Seiki M, Granato M, Hammerschmidt M, Heisenberg CP, Jiang YJ, Kane DA, Kelsh RN, Mullins MC, Nusslein-Volhard C.** 1996. Mutations affecting the cardiovascular system and other internal organs in zebrafish. Development **123:**293–302.
10. **Chenna R, Sugawara H, Koike T, Lopez R, Gibson TJ, Higgins DG, Thompson JD.** 2003. Multiple sequence alignment with the Clustal series of programs. Nucleic Acids Res **31:**3497–3500.
11. **Chicoine J, Benoit P, Gamberi C, Paliouras M, Simonelig M, Lasko P.** 2007. Bicaudal C recruits CCR4–NOT deadenylase to target mRNAs and regulates oogenesis, cytoskeletal organization, and its own expression. Dev Cell **13:**691–704.
12. **Clamp M, Cuff J, Searle SM, Barton GJ.** 2004. The Jalview Java alignment editor. Bioinformatics **20:**426–427.
13. **Cogswell C, Price SJ, Hou X, Guay-Woodford LM, Flaherty L, Bryda EC.** 2003. Positional cloning of *jcpk/bpk* locus of the mouse. Mamm Genome **14:**242–249.
14. **Cooper B.** 2000. Autosomal dominant polycystic kidney disease in Persian cats. Feline Pract **28:**20–21.
15. **Davenport JR, Watts AJ, Roper VC, Croyle MJ, van Groen T, Wyss JM, Nagy TR, Kesterson RA, Yoder BK.** 2007. Disruption of intraflagellar transport in adult mice leads to obesity and slow-onset cystic kidney disease. Curr Biol **17:**1586–1594.
16. **Davenport JR, Yoder BK.** 2005. An incredible decade for the primary cilium: a look at a once-forgotten organelle. Am J Physiol Renal Physiol **289:**F1159–F1169.
17. **de Castro E, Sigrist CJ, Gattiker A, Bulliard V, Langendijk-Genevaux PS, Gasteiger E, Bairoch A, Hulo N.** 2006. ScanProsite: detection of PROSITE signature matches and ProRule-associated functional and structural residues in proteins. Nucleic Acids Res **34:**W362-W365.
18. **Dent JA, Polson AG, Klymkowsky MW.** 1989. A whole-mount immunocytochemical analysis of the expression of the intermediate filament protein vimentin in *Xenopus*. Development **105:**61–74.
19. **Drummond IA.** 2000. The zebrafish pronephros: a genetic system for studies of kidney development. Pediatr Nephrol **14:**428–435.
20. **Drummond IA.** 2005. Kidney development and disease in the zebrafish. J Am Soc Nephrol **16:**299–304.
21. **Drummond IA, Majumdar A, Hentschel H, Elger M, Solnica-Krezel L, Schier AF, Neuhauss SC, Stemple DL, Zwartkruis F, Rangini Z, Driever W, Fishman MC.** 1998. Early development of the zebrafish pronephros and analysis of mutations affecting pronephric function. Development **125:**4655–4667.
22. **Finn RD, Mistry J, Schuster-Bockler B, Griffiths-Jones S, Hollich V, Lassmann T, Moxon S, Marshall M, Khanna A, Durbin R, Eddy SR, Sonnhammer EL, Bateman A.** 2006. Pfam: clans, web tools, and services. Nucleic Acids Res **34:**D247–D251.
23. **Flaherty L, Bryda EC, Collins D, Rudofsky U, Montogomery JC.** 1995. New mouse model for polycystic kidney disease with both recessive and dominant gene effects. Kidney Int **47:**552–558.
24. **Gabow PA.** 1993. Autosomal dominant polycystic kidney disease. N Engl J Med **329:**332–342.
25. **Gasteiger E, Gattiker A, Hoogland C, Ivanyi I, Appel RD, Bairoch A.** 2003. ExPASy: the proteomics server for in-depth protein knowledge and analysis. Nucleic Acids Res **31:**3784–3788.
26. **Golling G, Amsterdam A, Sun Z, Antonelli M, Maldonado E, Chen W, Burgess S, Haldi M, Artzt K, Farrington S, Lin SY, Nissen RM, Hopkins N.** 2002. Insertional mutagenesis in zebrafish rapidly identifies genes essential for early vertebrate development. Nat Genet **31:**135–140.
27. **Guay-Woodford LM.** 2006. Renal cystic diseases: diverse phenotypes converge on the cilium–centrosome complex. Pediatr Nephrol **21:**1369–1376.
28. **Hostetter CL, Sullivan-Brown JL, Burdine RD.** 2003. Zebrafish pronephros: a model for understanding cystic kidney disease. Dev Dyn **228:**514–522.
29. **Hou X, Mrug M, Yoder BK, Lefkowitz EJ, Kremmidiotis G, D'Eustachio P, Beier DR, Guay-Woodford LM.** 2002. Cystin, a novel cilia-associated protein, is disrupted in the *cpk* mouse model of polycystic kidney disease. J Clin Invest **109:**533–540.
30. **Huang H, Zhang B, Hartenstein PA, Chen JN, Lin S.** 2005. NXT2 is required for embryonic heart development in zebrafish. BMC Dev Biol **5:**7.
31. **Hulo N, Bairoch A, Bulliard V, Cerutti L, De Castro E, Langendijk-Genevaux PS, Pagni M, Sigrist CJ.** 2006. The PROSITE database. Nucleic Acids Res **34:**D227–D230.
32. **Igarashi P.** 2005. Overview: nonmammalian organisms for studies of kidney development and disease. J Am Soc Nephrol **16:**296–298.
33. **Institute of Laboratory Animal Resources.** 1996. Guide for the care and use of laboratory animals. Washington (DC): National Academies Press.
34. **Jones C, Roper VC, Foucher I, Qian D, Banizs B, Petit C, Yoder BK, Chen P.** 2008. Ciliary proteins link basal body polarization to planar cell polarity regulation. Nat Genet **40:**69–77.
35. **Karlstrom RO, Tyurina OV, Kawakami A, Nishioka N, Talbot WS, Sasaki H, Schier AF.** 2003. Genetic analysis of zebrafish *gli1* and *gli2* reveals divergent requirements for *gli* genes in vertebrate development. Development **130:**1549–1564.
36. **Kramer-Zucker AG, Olale F, Haycraft CJ, Yoder BK, Schier AF, Drummond IA.** 2005. Cilia-driven fluid flow in the zebrafish pronephros, brain and Kupffer's vesicle is required for normal organogenesis. Development **132:**1907–1921.
37. **Kugler JM, Chicoine J, Lasko P.** 2009. Bicaudal C associates with a trailer hitch–Me31B complex and is required for efficient gurken secretion. Dev Biol **328:**160–172.
38. **Li JB, Gerdes JM, Haycraft CJ, Fan Y, Teslovich TM, May-Simera H, Li H, Blacque OE, Li L, Leitch CC, Lewis RA, Green JS, Parfrey PS, Leroux MR, Davidson WS, Beales PL, Guay-Woodford LM, Yoder BK, Stormo GD, Katsanis N, Dutcher SK.** 2004. Comparative genomics identifies a flagellar and basal body proteome that includes the BBS5 human disease gene. Cell **117:**541–552.

39. **Liu S, Lu W, Obara T, Kuida S, Lehoczky J, Dewar K, Drummond IA, Beier DR.** 2002. A defect in a novel Nek-family kinase causes cystic kidney disease in the mouse and in zebrafish. Development **129:**5839–5846.
40. **Mahone M, Saffman EE, Lasko PF.** 1995. Localized bicaudal C RNA encodes a protein containing a KH domain, the RNA binding motif of FMR1. EMBO J **14:**2043–2055.
41. **Menezes LF, Cai Y, Nagasawa Y, Silva AM, Watkins ML, Da Silva AM, Somlo S, Guay-Woodford LM, Germino GG, Onuchic LF.** 2004. Polyductin, the PKHD1 gene product, comprises isoforms expressed in plasma membrane, primary cilium, and cytoplasm. Kidney Int **66:**1345–1355.
42. **Mercer EH.** 1963. A scheme for section staining in electron microscopy. J R Microsc Soc **81:**179–183.
43. **Nasevicius A, Ekker SC.** 2000. Effective targeted gene 'knockdown' in zebrafish. Nat Genet **26:**216–220.
44. **Obara T, Mangos S, Liu Y, Zhao J, Wiessner S, Kramer-Zucker AG, Olale F, Schier AF, Drummond IA.** 2006. Polycystin 2 immunolocalization and function in zebrafish. J Am Soc Nephrol **17:**2706–2718.
45. **Otto EA, Schermer B, Obara T, O'Toole JF, Hiller KS, Mueller AM, Ruf RG, Hoefele J, Beekmann F, Landau D, Foreman JW, Goodship JA, Strachan T, Kispert A, Wolf MT, Gagnadoux MF, Nivet H, Antignac C, Walz G, Drummond IA, Benzing T, Hildebrandt F.** 2003. Mutations in INVS encoding inversin cause nephronophthisis type 2, linking renal cystic disease to the function of primary cilia and left–right axis determination. Nat Genet **34:**413–420.
46. **Pagni M, Ioannidis V, Cerutti L, Zahn-Zabal M, Jongeneel CV, Falquet L.** 2004. MyHits: a new interactive resource for protein annotation and domain identification. Nucleic Acids Res **32:**W332-W335.
47. **Pathak N, Obara T, Mangos S, Liu Y, Drummond IA.** 2007. The zebrafish *fleer* gene encodes an essential regulator of cilia tubulin polyglutamylation. Mol Biol Cell **18:**4353–4364.
48. **Rozen S, Skaletsky H.** Primer3 on the WWW for general users and for biologist programmers. In: Krawetz S, Misener S, editors. Bioinformatics: methods and protocols. Totowa (NJ): Humana Press.
49. **Saffman EE, Styhler S, Rother K, Li W, Richard S, Lasko P.** 1998. Premature translation of oskar in oocytes lacking the RNA-binding protein bicaudal C. Mol Cell Biol **18:**4855–4862.
50. **Schultz J, Ponting CP, Hofmann K, Bork P.** 1997. SAM as a protein interaction domain involved in developmental regulation. Protein Sci **6:**249–253.
51. **Siroky BJ, Guay-Woodford LM.** 2006. Renal cystic disease: the role of the primary cilium–centrosome complex in pathogenesis. Adv Chronic Kidney Dis **13:**131–137.
52. **Snee MJ, Macdonald PM.** 2009. Bicaudal C and trailer hitch have similar roles in *gurken* mRNA localization and cytoskeletal organization. Dev Biol **328:**434–444.
53. **Stagner EE, Bouvrette DJ, Cheng J, Bryda EC.** 2009. The polycystic kidney disease-related proteins Bicc1 and SamCystin interact. Biochem Biophys Res Commun **383:**16–21.
54. **Sun Z, Amsterdam A, Pazour GJ, Cole DG, Miller MS, Hopkins N.** 2004. A genetic screen in zebrafish identifies cilia genes as a principal cause of cystic kidney. Development **131:**4085–4093.
55. **Takeyasu K, Tamkun MM, Renaud KJ, Fambrough DM.** 1988. Ouabain-sensitive (Na^{++} K^{+})-ATPase activity expressed in mouse L cells by transfection with DNA encoding the α subunit of an avian sodium pump. J Biol Chem **263:**4347–4354.
56. **Taulman PD, Haycraft CJ, Balkovetz DF, Yoder BK.** 2001. Polaris, a protein involved in left–right axis patterning, localizes to basal bodies and cilia. Mol Biol Cell **12:**589–599.
57. **Tran U, Pickney LM, Ozpolat BD, Wessely O.** 2007. *Xenopus* bicaudal C is required for the differentiation of the amphibian pronephros. Dev Biol **307:**152–164.
58. **Tran U, Zakin L, Schweickert A, Agrawal R, Blum M, De Robertis EM, Wessely O.** 2009. The role of bicaudal C in kidney development. Mech Dev **126:**S159.
59. **Wessely O, De Robertis EM.** 2000. The *Xenopus* homologue of bicaudal C is a localized maternal mRNA that can induce endoderm formation. Development **127:**2053–2062.
60. **Wessely O, Obara T.** 2008. Fish and frogs: models for vertebrate cilia signaling. Front Biosci **13:**1866–1880.
61. **Westerfield M**. The zebrafish book: a guide for the laboratory use of zebrafish *Danio* (*Brachydanio*) *rerio*. Eugene (OR): Institute of Neuroscience, University of Oregon.
62. **Wilson PD.** 2004. Polycystic kidney disease. N Engl J Med **350:**151–164.
63. **Winkelbauer ME, Schafer JC, Haycraft CJ, Swoboda P, Yoder BK.** 2005. The *C. elegans* homologs of nephrocystin 1 and nephrocystin 4 are cilia transition-zone proteins involved in chemosensory perception. J Cell Sci **118:**5575–5587.
64. **Yoder BK.** 2007. Role of primary cilia in the pathogenesis of polycystic kidney disease. J Am Soc Nephrol **18:**1381–1388.
65. **Yoder BK, Tousson A, Millican L, Wu JH, Bugg CE Jr, Schafer JA, Balkovetz DF.** 2002. Polaris, a protein disrupted in *orpk* mutant mice, is required for assembly of renal cilium. Am J Physiol Renal Physiol **282:**F541–F552.
66. **Zdobnov EM, Apweiler R.** 2001. InterProScan—an integration platform for the signature-recognition methods in InterPro. Bioinformatics **17:**847–848.
67. **Zhang Q, Taulman PD, Yoder BK.** 2004. Cystic kidney diseases: all roads lead to the cilium. Physiology (Bethesda) **19:**225–230.